

FLOW AND ACOUSTICS BY SHOCK-TURBULENCE INTERACTION IN TWIN-JETS CONFIGURATION

Aatresh Karnam and Ephraim Gutmark
Department of Aerospace Engineering & Engineering Mechanics
University of Cincinnati, Cincinnati, Ohio, USA.

Instability states in twin square jets at off-design conditions are investigated in this study. Experimental datasets from Schlieren imaging supplemented with Particle Image Velocimetry data were analyzed to identify and isolate various instability modes. It was observed that Twin square jets undergo a wide range of inter-jet coupling modes driven by shock-turbulence interactions. These interactions result in two distinct types of instability modes. The first mode consisted of phase locked inner shear layers oscillating in conjunction with the outer shear layers, while the second mode resulted in phase locked inner shear layers oscillating at a phase separation of $\pi/2$ radians to the outer shear layers. Furthermore, the former mode propagated into both nozzle orientation planes while the latter mode was observed to be dominant primarily in the twin-jet plane.

I. Introduction

Increasing competition in the private orbital launch sectors has led to the development of large multi-nozzle launch vehicles such as the Super Heavy, first stage booster of the Space X Starship consisting of 33 circular nozzles. While conventional circular nozzles offer the advantage of being a tried and tested design, they can require complex vectoring systems to steer launch vehicles. On the contrary non-circular symmetric geometries such as square nozzles require simpler vectoring systems similar to those used on the Lockheed Martin/Boeing F-22 Raptor. These nozzles can also offer better packaging patterns in the context of multi-nozzle configurations similar to that used in the Super Heavy booster. While extensive studies have been undertaken exploring the flow characteristics of rectangular nozzles [1]–[11], far less is understood about square nozzle geometries owing to fewer studies on these nozzles [12]. While the work by Karnam et al. [13] and Ahn et al. [14], [15] focused on instability characteristics of twin square nozzles at the overexpanded state of NPR 3, the aim of this study is to further explore design and off design behavior of this geometry and document the various interaction modes that can occur between the jets. As such, some of the results discussed there have been utilized to provide a holistic understanding of jet interactions.

II. Experimental Setup & Analysis Techniques

All experiments were conducted on the Heated Jet Noise Rig (HJNR) located in the Gas Dynamics and Propulsion Lab at the University of Cincinnati. The facility consists of a state-of-the-art anechoic chamber with a design noise floor of 300Hz to minimize acoustic noise due to reflections. Apart from noise measurements, the facility is also equipped for qualitative data analysis in the form of Particle Image Velocimetry (PIV) as well as quantitative flow analysis through high speed Schlieren image capture (up to 200kHz). The details of the nozzle geometry as well as the flow measurement techniques are discussed below.

A. Nozzle Geometry

The geometry consists of twin nozzle setup with square exit planes of height $h = 16.61$ mm with a separation of $2.12 h$ between the nozzle centerlines. Each nozzle consisting of a convergent divergent section and a flat section as shown in Fig. 1. Also seen are the two measurement planes, the C – D Plane (XY) passing through the center of the convergent divergent section of each nozzle and the Flat Plane (XZ) perpendicular to the flat faces of both the nozzles. The nozzles are designed for $M_{design} = 1.5$ at $NPR = 3.67$. The nozzles receive air from a common plenum that is split into individual streams via a contoured splitter designed with a polynomial profile to avoid flow separation. A straight section $2.64 h$ in length is placed before the C – D section to streamline the flow & minimize the formation of a skewed velocity gradient across the jet.

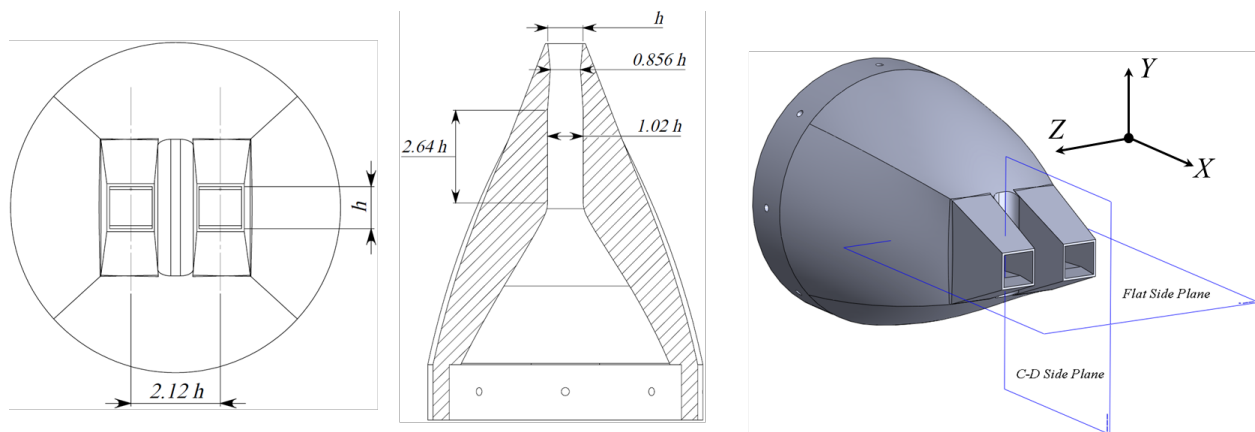


Figure 1. Twin square nozzle geometry. a) Top view. b) Sectional view along the center plane of one of the nozzles. c) Measurement plane & nozzle orientation axes.

B. Particle Image Velocimetry (PIV) Setup

PIV images were acquired using a pair of LaVision Imager Intense CCD cameras, each with a 1376×1040 pixel array (pixel pitch: $6.45 \mu\text{m}$) stacked vertically as seen below in Fig. 1. An Evergreen Dual Pulse Nd: Yag laser operating at a peak frequency of 5Hz at 532 nm (170mJ per pulse) was used for illumination. The laser beam was passed through an iris to minimize distortion effects due to non – circular beam cross – section, then through a focusing lens & finally a cylindrical lens to produce a sheet $\approx 1\text{mm}$ in thickness. The two cameras were paired with Nikon (NIKKOR) 50mm lenses at $f/16$ aperture to maximize the measurement area. An optical bandpass filter (Wavelength: 532 nm; Optical Density: 6; Full – Width Half Max (FWHM): $\pm 10\text{nm}$) was used with each lens to avoid capturing light from surface/stray reflections without affecting the light reflected off the seed particles. A knife edge was also used to limit the spread of the laser sheet which can cause strong reflections from the nozzle lip bleeding into the camera frame. The choice of the lens was made to accommodate both the jets in the Twin Jet configuration. The camera & the laser were synchronized through a LaVision Programmable Timing Unit (PTU) with control & measurements made using LaVision DaVis 8.4 software. The interval between successive frames was set to $0.5 \mu\text{s}$ to minimize measurement lag given the large FOV provided by the lens. For each test condition a series of 1200 images are recorded for vector field & flow property computation.

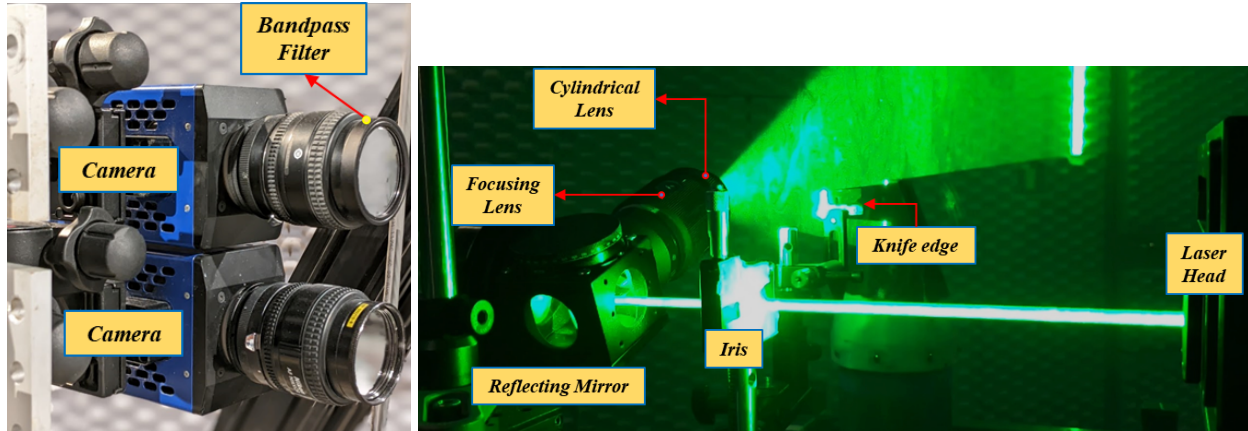


Figure 2. PIV setup for image capture. a) Camera set up and orientation. b) Laser optics for illumination.

The camera – lens combination resulted in a magnification of 12.55 pixels(px)/mm with a pixel shift of 2.33 px at 370 m/s (NPR 2.5) & 2.7 px at 430 m/s (NPR 3.67). Table 1 shows some of the crucial PIV parameters. Details regarding validation of the PIV setup are discussed in detail in [13]. The final images obtained after post-processing have a vector resolution of 174 x 132 vectors per image frame.

Table 1 – PIV Parameters

Parameter	Value
Interrogation window – Initial pass (px)	128 x 128
Interrogation window – Final pass (px)	16 x 16
Interrogation window – Final (Det)	0.07 x 0.07
Overlap %	50
Frame separation (μ s)	0.5
Exposure time (ns)	500
Field of View (Det)	5.92 x 4.48
Digital Resolution (px/Det)	231.6

C. Schlieren & Near Field Microphone Setup

The schlieren setup consists of a single parabolic mirror (focal length (f_{mirror}) = 1.8 m) and a light source separated by a distance of $2f_{\text{mirror}}$ as detailed in Settles [24]. The choice of the setup was constrained by the chamber & jet layout ruling out the possibility of the more commonly used Z – type schlieren setup. Images were captured using a Vison Research Phantom v1610 capable of recording up to a frame rate of 204,800 Hz with an exposure of 10μ s. Illumination was provided using an Oriel High Intensity UV light source operating continuously at 50 – 200W. The light was passed through a collimating lens & an iris to create a point source of light before being passed through a beam splitter to filter out the source & image light rays that are reflected from the mirror after passing through the jet. The reflected beam is then cut using a horizontal knife edge (oriented perpendicular to the flow direction) to highlight the features in the jet and the acoustic waves propagating in the ambient. A Nikon AF 300 mm lens is used for proper focus and image capture as seen in Fig. 3(a). Due to the nature of the single mirror set up, the scale of the jet is slightly reduced (1:1.2) when compared to a Z – type set up where a 1:1 scaling is possible. To account for this magnification and scaling effects images are

recorded using LaVision Davis 8.4 after proper calibration. An array of six near field Brüel & Kjaer quarter inch microphones was used to capture simultaneous acoustics along with the schlieren images as shown in Fig. 3(b). The data was recorded at an acquisition rate of 204,800 Hz for a duration of 2 seconds. Data recording was triggered by a LaVision PTU – X timings unit that simultaneously triggered the microphones & the high-speed camera while maintaining minimum latency.

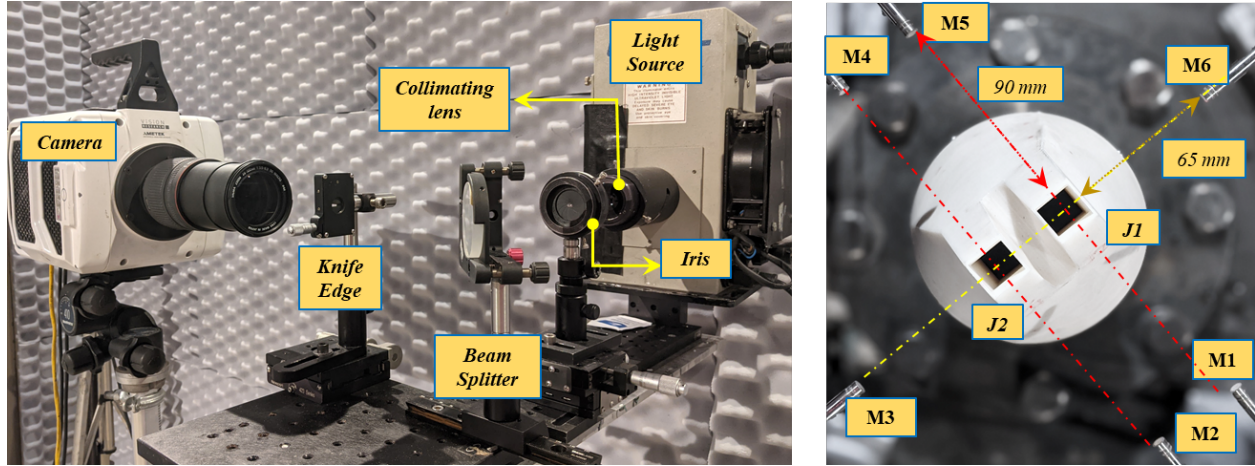


Figure 3. a) Optical elements used for high speed Schlieren image capture. b) Near field microphone array used for simultaneous noise measurement.

III. Results & Discussion

A. Acoustic Results

Figure 4 shows the results obtained from the near field acoustic data from opposing microphone locations. An approximate linear trend with decreasing values of the peak instability frequency was observed across the range of operating conditions of the nozzle from NPR 2.5 – NPR 4.5 as seen in Fig. 4(a) at the microphones locations M1, M3 placed normal to the twin jet plane (Fig. 3(b)). This is expected as an increase in the nozzle inlet pressure leads to an increase in shock cell width thus lowering the frequency of oscillation [11].

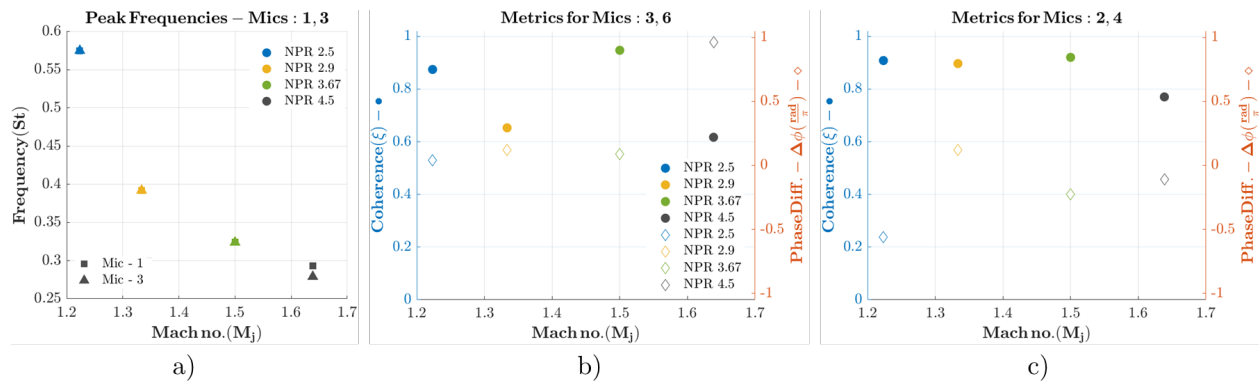


Figure 4. a) Peak instability frequency variation with nozzle Mach no. captured at M1(C – D Plane) & M3 (Twin jet Plane). b) Phase and coherence vs Mach no. at peak frequency for mics M3, M6. c) Phase and coherence vs Mach no. at peak frequency for mics M2, M4.

While the trend of peak frequencies is predictable, the oscillation phase at these frequencies was found to vary considerably depending on the observation plane. In the case of acoustics propagating in the twin jet plane the phase difference remains invariant for NPR 2.5, 2.9 and 3.67 while the underexpanded case of NPR 4.5 showed a phase difference of π radians between the outer shear layers as seen in Fig. 4(b). The trend in the case of mics M2, M4 in the C-D plane of the nozzles is far less predictable with changes in the phase difference being sporadic. This indicates that the instabilities generated in the nozzle propagate primarily in the twin jet plane with lower directional preference given to the C-D plane. This is also evident in the spectrograms obtained for M1, M3 for NPR 2.9 and NPR 4.5 as seen in Fig. 5. In the case of NPR 2.9, shown in Fig. 5(a), (b), the twin jets undergo strong screeching behavior with prominent propagation of the primary tone ($St = 0.38$) and its harmonic in the twin jet plane capture in M3, while M1 only receives weak acoustic tones at these frequencies. In the case of NPR 4.5, the disparity, while not as severe, is still observable. Clear instability tones were detected in the data from M3, while M1 was dominated primarily by the Broad Band Shock Associated Noise (BBSN) as seen in Fig. 5(c), (d).

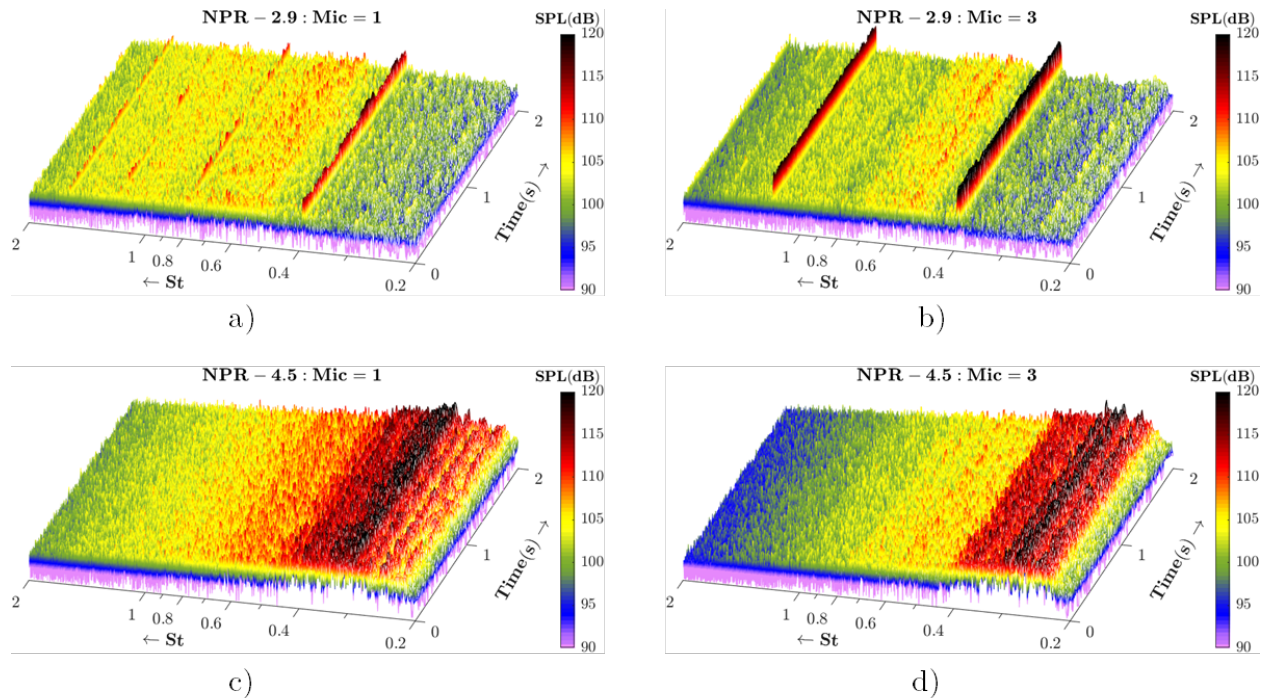


Figure 5. a) Peak instability frequency variation with nozzle Mach no. captured at M1(C – D Plane) & M3 (Twin jet Plane). b) Phase and coherence vs Mach no. at peak frequency for mics M3, M6. c) Phase and coherence vs Mach no. at peak frequency for mics M2, M4.

B. Schlieren Results

The high acquisition rate of the Phantom led to a wide Nyquist cut-off frequency ranging from 20.5kHz to 102.4kHz based on the initial acquisition rate. These images were utilized as input for Spectral Proper Orthogonal Decomposition (SPOD) developed by Schmidt and Colonius[16] allowing for a wide range of frequencies to identify instability modes. The SPOD technique allows for filtering of the total energy content of the flow into spatial energy modes in descending order of energy along with spectral decomposition from temporal to frequency

domain. This aids in pinpointing the spatial energy distribution associated with the spectral peaks observed in the near field acoustic data. Figure 6 shows the temporal average of the Schlieren images from an observation point normal to the twin jet plane, the energy spectra from the SPOD analysis and the primary instability mode. Also marked are the spectra from the near field microphone M2 placed normal to the twin jet plane as a frequency reference.

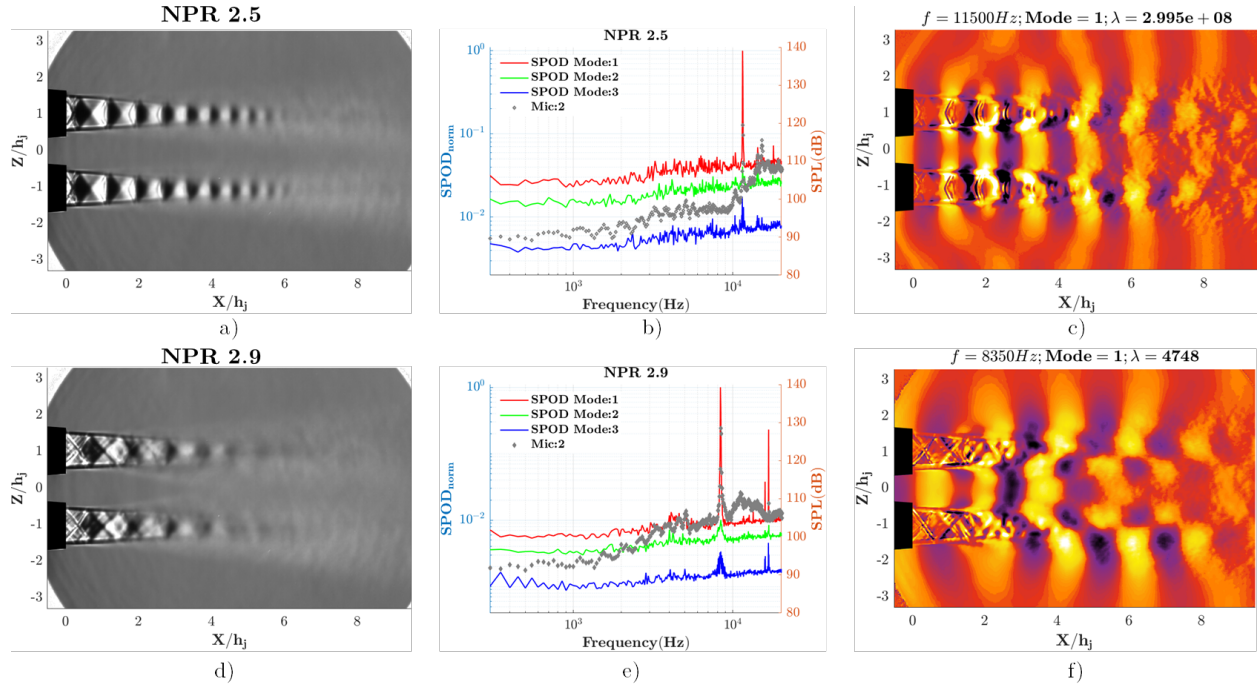


Figure 6. a) Temporal average of Schlieren images, energy spectra from SPOD analysis and the primary instability mode in the twin jet plane for NPR 2.5: a) – c) and NPR 2.9: d) – f).

In the case of NPR 2.5, the twin jets are in the overexpanded state leading to the formation of a clear shock train initiated by a Mach disk that forms at $X/h_j \approx 1$ from the nozzle exit extending up to $X/h_j \approx 7$ as seen in Fig. 6(a). The SPOD energy spectra and the acoustic spectra both show a clear peak at 11.5kHz indicating the presence of an oscillating jet mode as observed in Fig. 6(b). The spatial energy distribution of the SPOD mode at this frequency reveals a strong symmetric instability mode as seen in Fig. 6(c). All the shear layers (inner and outer) oscillate in the same phase. This result agrees with the trend observed in the acoustic results discussed in Section III A and seen in Fig. 4(b). Furthermore, the phase offset of $\pi/2$ observed across microphones M2 and M4 indicates that the twin jets also have a simultaneous oscillation amplitude mode normal to the twin jet plane at this frequency.

When the operating condition of the jet was shifted to NPR 2.9, the amplitude of jet oscillations in the twin jet plane increased significantly leading to the development of a strong flapping motion. This led to significant smearing of the shock structure of the jets in the temporal Schlieren average as seen in Fig. 6(d). The acoustic peak resulting from the flapping mode was recorded at 8.35kHz as seen in the acoustics and SPOD spectra shown in Fig. 6(e). The trend observed in Fig. 4(b) indicated that the outer shear layers were phase matched for NPR 2.9 similar to the result observed for NPR 2.5. However, while this is true, the inner shear layers

were found to be phase locked and oscillated at a phase difference of $\pi/2$ radians compared to the outer shear layers as seen in Fig. 6(f).

This change in oscillation mode indicates that the jets show mirror symmetry with the jet symmetry line as the mirror plane. Additionally, while the jets undergo multi-plane oscillations at NPR 2.5, jet fluctuations were limited to the twin jet plane in the case of NPR 2.9.

IV. Future Work

This abstract briefly discusses the techniques and a few of the results obtained from experiments. The authors are currently analyzing a large amount of experimental data and intend to elucidate them in greater detail in the long form publication. Those would also include results from PIV experiments across both planes of observation (twin jet plane, C-D plane).

V. Acknowledgement

The authors would like to thank & acknowledge Dr. Steve Martens and The Office of Naval Research (ONR) for their continued support and funding (Grant Nos: N00014-18-1-2582; N00014-18-1-2391) without which this research could not have taken form.

VI. References

- [1] M. B. Alkisar, A. Krothapalli, and L. M. Lourenco, "Structure of a screeching rectangular jet: a stereoscopic particle image velocimetry study," *J. Fluid Mech.*, vol. 489, pp. 121–154, Jul. 2003, doi: 10.1017/S0022112003005032.
- [2] A. Krothapalli, D. Baganoff, and K. Karamcheti, "On the mixing of a rectangular jet," *J. Fluid Mech.*, vol. 107, no. 1, p. 201, Jun. 1981, doi: 10.1017/S0022112081001730.
- [3] A. Krothapalli, Y. Hsia, D. Baganoff, and K. Karamcheti, "The role of screech tones in mixing of an underexpanded rectangular jet," *Journal of Sound and Vibration*, vol. 106, no. 1, pp. 119–143, Apr. 1986, doi: 10.1016/S0022-460X(86)80177-8.
- [4] K. Viswanath et al., "Flow Statistics and Noise of Ideally Expanded Supersonic Rectangular and Circular Jets," *AIAA Journal*, vol. 55, no. 10, pp. 3425–3439, Oct. 2017, doi: 10.2514/1.J055717.
- [5] K. Viswanath, J. Liu, R. Ramamurti, A. Karnam, F. Baier, and E. J. Gutmark, "Noise Characteristics of Low Aspect Ratio Supersonic Twin Jet Configuration," in *AIAA Scitech 2020 Forum*, Orlando, FL: American Institute of Aeronautics and Astronautics, Jan. 2020. doi: 10.2514/6.2020-0496.
- [6] J. Jeun, A. Karnam, G. Jun Wu, S. K. Lele, F. Baier, and E. J. Gutmark, "Aeroacoustics of Twin Rectangular Jets Including Screech: Large-Eddy Simulations with Experimental Validation," *AIAA Journal*, vol. 60, no. 11, pp. 6340–6360, Nov. 2022, doi: 10.2514/1.J060895.
- [7] B. Malla, J. Holder, V. Anand, and E. Gutmark, "Structural excitation of SERNs during supersonic operation: A source of screech amplitude modulation," *Journal of Fluids and Structures*, vol. 107, p. 103390, Nov. 2021, doi: 10.1016/j.jfluidstructs.2021.103390.
- [8] B. Semlitsch, B. Malla, E. J. Gutmark, and M. Mihăescu, "The generation mechanism of higher screech tone harmonics in supersonic jets," *J. Fluid Mech.*, vol. 893, p. A9, Jun. 2020, doi: 10.1017/jfm.2020.233.

- [9] F. Baier, A. Karnam, and E. Gutmark, “Cold Flow Measurements of Supersonic Low Aspect Ratio Jet-Surface Interactions,” *Flow Turbulence Combust*, vol. 105, no. 1, pp. 1–30, Jun. 2020, doi: 10.1007/s10494-019-00098-w.
- [10] A. Karnam, F. Baier, E. J. Gutmark, J. Jeun, G. J. Wu, and S. K. Lele, “An Investigation into Flow Field Interactions between Twin Supersonic Rectangular Jets,” in *AIAA Scitech 2021 Forum*, in *AIAA SciTech Forum*. , American Institute of Aeronautics and Astronautics, 2021. doi: 10.2514/6.2021-1291.
- [11] A. Karnam, M. Saleem, and E. Gutmark, “Influence of nozzle geometry on screech instability closure,” *Physics of Fluids*, vol. 35, no. 8, p. 086119, Aug. 2023, doi: 10.1063/5.0161032.
- [12] D. Zilz and R. Wlezien, “The sensitivity of near-field acoustics to the orientation of twin two dimensional supersonic nozzles,” in *26th Joint Propulsion Conference*, Orlando, FL, U.S.A.: American Institute of Aeronautics and Astronautics, Jul. 1990. doi: 10.2514/6.1990-2149.
- [13] A. Karnam, M. Ahn, E. Gutmark, and M. Mihaescu, “Effects of Screech on Jet Coupling in Twin Square Jets,” in *28th AIAA/CEAS Aeroacoustics 2022 Conference*, in *Aeroacoustics Conferences*. American Institute of Aeronautics and Astronautics, 2022. doi: 10.2514/6.2022-3067.
- [14] M. Ahn, A. Karnam, E. Gutmark, and M. Mihaescu, “Flow and Near-field Pressure Fluctuations of Twin Square Jets,” in *AIAA Propulsion and Energy 2021 Forum*, VIRTUAL EVENT: American Institute of Aeronautics and Astronautics, Aug. 2021. doi: 10.2514/6.2021-3554.
- [15] M. Ahn, M. Mihaescu, A. Karnam, and E. Gutmark, “Large-eddy simulations of flow and aeroacoustics of twin square jets including turbulence tripping,” *Physics of Fluids*, vol. 35, no. 6, p. 066105, Jun. 2023, doi: 10.1063/5.0147295.
- [16] O. T. Schmidt and T. Colonius, “Guide to Spectral Proper Orthogonal Decomposition,” *AIAA Journal*, vol. 58, no. 3, pp. 1023–1033, Mar. 2020, doi: 10.2514/1.J058809.